

Mechanisms of Transcriptional Silencing by the
Nuclear Piwi Protein in *Drosophila* Germ Cells

Supplemental Material

Thesis by
Alicia Kathryn Rogers

In Partial Fulfillment of the Requirements for the
degree of
Doctor of Philosophy in Biology

Caltech

CALIFORNIA INSTITUTE OF TECHNOLOGY

Pasadena, California

2018
(Defended March 29, 2018)

© 2018

Alicia Kathryn Rogers
ORCID: 0000-0001-5525-6095

TABLE OF CONTENTS

Table of Contents.....	iii
List of Illustrations and/or Tables	iv
Chapter II. Piwi induces piRNA-guided transcriptional silencing and establishment of a repressive chromatin state Supplemental material.....	1
Supplementary Methods	1
Supplementary References.....	4
Supplementary Tables.....	5
Supplementary Figures and Figure Legends	11
Chapter III. piRNA-independent recruitment of Piwi to RNA transcripts is not sufficient to trigger transcriptional silencing.....	16
Supplementary Tables.....	16
Chapter IV. Zucchini-dependent piRNA processing is triggered by recruitment to the cytoplasmic processing machinery Supplemental Material	17
Supplementary Tables.....	18
Supplementary Figures and Figure Legends	20
Chapter V. Identifying direct protein interactions with Piwi using a heterologous cell culture assay Supplemental Material.....	26
Supplementary Tables.....	1
Supplementary Figures and Figure Legends	2

LIST OF ILLUSTRATIONS AND/OR TABLES

	<i>Page</i>
Chapter II	
Supplementary Table 1. List of genes significantly upregulated upon Piwi knockdown.....	5
Supplementary Table 2. PCR primers.....	8
Supplementary Table 3. ChIP-seq datasets read mapping statistics.....	8
Supplementary Table 6. Repeat analysis mapping statistics. (consensus sequences).....	10
Supplementary Figure S1. Fluorescence Loss in Photobleaching (FLIP) experiments indicate fast redistribution of most of nuclear Piwi and slower movement of the Piwi-YK mutant.....	11
Supplementary Figure S2. Piwi regulates transposon levels through transcriptional repression.....	12
Supplementary Figure S3. Piwi depletion increases RNA Pol II association with promoters of transposable elements.....	14
Supplementary Figure S4. Piwi depletion does not alter H3K9me3 occupancy over differentially expressed genes upon Piwi knockdown.....	15
Chapter III	
Supplementary Table S1. Oligonucleotide sequences used in experimental procedures ...	16
Chapter IV	
Supplementary Table S1. Library mapping statistics.....	18
Supplementary Table S2. Oligonucleotide sequences used in experimental procedures. ...	19
Supplementary Figure S1. Upon Zuc tethering, reporter derived sequences that are 25-28nt in length (black) map along the whole body of the reporter, whereas 22-23nt reads (red) map predominantly at the 5' region of the reporter transcript.....	20
Supplementary Figure S2. Recruitment of Piwi to the reporter triggers production of piRNAs in sense orientation.....	21
Supplementary Figure S3. Production of piRNAs upon Piwi tethering is independent of the λ N-Piwi fusion construct, as well as the reporter sequence and genomic location.....	22
Supplementary Figure S4. Recruitment of Piwi, Aub, or Armi to the reporter triggers production of piRNAs resistant to NaIO ₄ treatment	24
Supplementary Figure S5. Percent mRNA remaining after knockdown of piRNA pathway component mRNAs in the tethering system.....	25
Chapter V	
Supplementary Table S1. Colocalization analysis statistics.....	1
Supplementary Table S2. Oligonucleotide sequences used in experimental procedures.	1
Supplementary Figure S1. Piwi does not directly interact with many nuage localized factors involved in piRNA biogenesis.	2
Supplementary Figure S2. Piwi does not directly interact with several factors involved in transcript export from the nucleus.....	4
Supplementary Figure S3. Piwi does not directly interact with many nuclear factors involved in chromatin modification.	5

Chapter II

PIWI INDUCES PIRNA-GUIDED TRANSCRIPTIONAL SILENCING AND ESTABLISHMENT OF A REPRESSIVE CHROMATIN STATE SUPPLEMENTAL MATERIAL

This work was first published as:

Le Thomas, A. et al. (2013). "Piwi induces piRNA-guided transcriptional silencing and establishment of a repressive chromatin state". In: *Genes & Development* 27: 390-399. doi: 10.1101/gad.209841.112.

Supplementary Methods

High throughput data analysis:

Except for where specifically specified otherwise, all data processing was carried out using custom-written python scripts. The dm3/BDGP assembly, release 5 version of the Drosophila melanogaster genome was used.

ChIP-seq and ChIP-seq data processing:

Sequencing libraries were sequenced on the Illumina HiSeq 2000 (50bp reads). The resulting sequencing reads were trimmed down to 36bp and mapped against the genome using Bowtie 0.12.7 (Langmead et al. 2009) with the following settings: "-v 2 --best --strata" retaining only uniquely mappable reads with up to two mismatches. Read mapping statistics for ChIP-seq datasets processed this way are presented in Supplementary Table 3.

Gene expression quantification using RNA-seq:

RNA-seq libraries were built from polyA-selected RNA from fly ovaries following standard protocols (Mortazavi et al. 2008) and sequenced on the HiSeq 2000 (50bp reads). For the purposes of expression quantification, reads were mapped as 50mers, using TopHat 1.4.1 (Trapnell et al. 2009) and splice junctions from the ENSEMBL62 dm3 annotation with otherwise default settings. Gene expression was quantified in RPKMs/FPKMs (Reads/Fragments Per Kilobase per Million mapped reads/fragments) for the refSeq annotation (downloaded from the UCSC browser) with

Cufflinks 2.0.2 (Trapnell et al. 2010; Trapnell et al. 2012). Read mapping statistics for these libraries are presented in Supplementary Table 4.

Repeats analysis:

The usual practice when mapping ChIP-seq data is to retain only unique alignments as the ambiguity of the allocation of multimapper seriously confounds most analyses. In this study it was necessary to examine repeats but not absolutely necessary to properly allocate multimappers to each individual repeat; we therefore adopted the following two strategies for processing our ChIP-seq and RNA-seq data and examining ChIP enrichment over the expression of repeat elements.

Repeats analysis on RepeatMasker-annotated repeat elements:

Both ChIP-seq and RNA-seq reads were trimmed down to the same length (36bp) and again aligned with Bowtie 0.12.7 against the dm3 genome but this time with the following options: "-v 0 -a --best --strata -q", i.e. no mismatches and an unlimited number of locations to which a read can map to. Read mapping statistics for these alignments are presented in Supplementary Table 5. For each read r , an integer multiplicity score NH_r was defined (corresponding to the number of positions in the genome the read maps to) and for each individual instance of a repeated element RE (as defined in the RepeatMasker repeat element annotation downloaded from UCSC) an RPM score was calculated as follows:

$$RPM_{RE} = \sum_{r \in RE} \frac{1}{NH_r}$$

For each repeat element in the RepeatMasker annotation, a combined RPM score over all its instances was calculated as the sum of the RPMs for each individual instance belonging to each group of elements in that level:

$$TotalRPM_{RE} = \sum_{RE} RPM_{RE}$$

Repeats analysis on consensus repeat sequences:

An orthogonal strategy for the analysis of repeat occupancy and expression change that we employed was to map reads against consensus repeat sequences (obtained from

FlyBase version FB2012_05 (McQuilton et al. 2012)). Reads were mapped with the following settings: "-v 3 -a --best --strata -q" (allowing for up to 3 mismatches and unlimited number of multimappers). Read mapping statistics for these alignments can be found in Supplementary Table 6. Read counts for each repeat were calculated (normalizing for multimapper multiplicity as described above) and normalized for sequencing depth against the total number of reads mappable to the genome (derived from the alignment without limits to read multiplicity discussed in the previous section) and finally, normalized for the length of the consensus sequences (RPKMs).

Differential expression and occupancy analysis

In order to identify differentially expressed genes and transposons we used a combination of eXpress quantification (Roberts and Pachter 2013) and DESeq (Anders and Huber 2010) differential read count analysis. For each replicate, RNA-seq reads were aligned against the transcriptome and the quantification values for all transcripts belonging to the same gene were summed to derive gene-level quantifications. The "eff_counts" values were used for downstream analysis. As only a minority of reads align to transposons, differential expression analysis only on transposons is not reliable. For this reason, we combined raw read counts for transposons (derived for the RepeatMasker annotation as described above or for the consensus sequences) with the eXpress quantifications on genes and ran DESeq to evaluate the statistical significance of the observed expression changes over the two shWhite and shPiwi replicates.

Differential occupancy of H3K9me3 was estimated as follows. First, the genome was divided into 1000bp bins and the H3K9me3 read count was estimated for each using the alignments generated with unlimited number of locations a read can map (dividing each alignment by the read multiplicity as discussed above). Next, DESeq was run on the H3K9me3 replicates to identify regions enriched or depleted upon Piwi knock down (p-value of 0.05 threshold was applied). Neighboring depleted regions were merged into contiguous clusters.

Pol II occupancy change over transposons was estimated from the combined RPM values for RepeatMasker transposons and from RPKM values for consensus transposons after taking into account that as the difference in ChIP signal between two regions is the result of the combination of the actual change in occupancy and the difference in ChIP

strength between the two experiments. We therefore used the total Pol II RPMs over TSSs in order to assess the difference in ChIP strength and derive a normalization factor to be used for rescaling of the repeat RPMs of libraries so that they are comparable to those in the other (this factor turned out to be close to 1 for both sets of replicates).

Supplementary References

- Anders S, Huber W. 2010. Differential expression analysis for sequence count data. *Genome biology* **11**: R106.
- Langmead B, Trapnell C, Pop M, Salzberg SL. 2009. Ultrafast and memory-efficient alignment of short DNA sequences to the human genome. *Genome biology* **10**: R25.
- McQuilton P, St Pierre SE, Thurmond J, FlyBase C. 2012. FlyBase 101--the basics of navigating FlyBase. *Nucleic acids research* **40**: D706-714.
- Mortazavi A, Williams BA, McCue K, Schaeffer L, Wold B. 2008. Mapping and quantifying mammalian transcriptomes by RNA-Seq. *Nature methods* **5**: 621-628.
- Roberts A, Pachter L. 2013. Streaming fragment assignment for real-time analysis of sequencing experiments. *Nature methods* **10**: 71-73.
- Trapnell C, Pachter L, Salzberg SL. 2009. TopHat: discovering splice junctions with RNA-Seq. *Bioinformatics* **25**: 1105-1111.
- Trapnell C, Roberts A, Goff L, Pertea G, Kim D, Kelley DR, Pimentel H, Salzberg SL, Rinn JL, Pachter L. 2012. Differential gene and transcript expression analysis of RNA-seq experiments with TopHat and Cufflinks. *Nature protocols* **7**: 562-578.
- Trapnell C, Williams BA, Pertea G, Mortazavi A, Kwan G, van Baren MJ, Salzberg SL, Wold BJ, Pachter L. 2010. Transcript assembly and quantification by RNA-Seq reveals unannotated transcripts and isoform switching during cell differentiation. *Nature biotechnology* **28**: 511-515.

Supplementary Tables

Supplementary Table 1. List of genes significantly upregulated upon Piwi knockdown.

Shown are the DESeq $\log_2(foldchange)$ and p-values as calculated from two biological replicates

Gene	$\log_2(foldchange)$	p-value
CG14628	Inf	6.77E-10
CG15056	Inf	8.05E-03
CG18823	Inf	2.77E-02
CG31054	Inf	3.28E-12
CG4984	Inf	2.59E-02
Sdic1	Inf	3.80E-02
yellow-c	Inf	9.49E-03
blanks	9.97	7.11E-04
Rpt6R	9.50	3.17E-05
CG32259	7.65	3.91E-02
Rpt3R	6.42	1.73E-07
Oseg5	6.32	8.24E-07
Shawl	6.10	2.02E-09
CG18193	5.63	1.56E-02
CG15201	5.37	4.01E-02
CG12493	5.24	1.87E-02
TrxT	5.19	5.90E-03
salt	5.14	4.61E-02
CG4650	4.74	2.73E-02
CR18854	4.59	3.91E-11
Rbp4	4.48	1.69E-03
PebIII	4.42	5.82E-03
CG5791	4.33	1.52E-02
CG13321	4.26	2.81E-09
CG3884	3.79	1.47E-02
CG12655	3.68	3.73E-03
CG10151	3.45	6.51E-05
CG5281	3.32	9.62E-05
GstD2	3.32	3.00E-02
CG30108	3.30	3.83E-06
IM1	3.30	1.59E-02
CG10440	3.23	2.18E-02
CG34291	3.20	3.13E-02
CG16758	3.14	1.34E-02
CG6776	3.10	3.14E-05
Cyp12d1-p	3.03	1.37E-03
CG18186	2.94	1.18E-05
Obp99b	2.86	5.56E-04
CG1600	2.82	2.48E-04
CG13936	2.79	4.55E-02
Hsp70Ab	2.77	7.62E-03
CG7470	2.70	2.51E-04
Gfat1	2.65	4.23E-03
CG9960	2.60	2.87E-03
Ptp52F	2.58	1.58E-03
GstD10	2.58	4.32E-02

Gene	$\log_2(foldchange)$	p-value
GstD5	2.57	2.29E-02
Mdr49	2.57	1.13E-02
Lsd-1	2.48	7.31E-04
scpr-A	2.47	3.65E-03
GstE5	2.45	3.60E-02
Cyp28d1	2.34	1.05E-02
CG7408	2.34	4.42E-02
CG9380	2.30	1.04E-02
CG15347	2.28	2.26E-02
CG14629	2.27	1.03E-02
CG32572	2.26	7.74E-03
CG5399	2.24	4.98E-03
Jheh3	2.20	8.99E-03
CG5171	2.19	3.17E-02
CG9743	2.17	4.68E-02
Hsp23	2.13	8.02E-04
RpS19b	2.10	4.61E-02
Lip4	2.07	6.69E-03
Hsp70Aa	2.06	8.74E-05
IM2	2.05	3.62E-02
Pomp	2.00	8.31E-04
pncr008	1.99	4.42E-03
CG5853	1.96	1.08E-02
CG9360	1.93	2.94E-02
CG30104	1.93	5.42E-03
CG12290	1.92	2.58E-02
ref(2)P	1.92	1.26E-03
Prosalpha5	1.92	1.56E-03
CR42871	1.91	3.78E-02
Pros28.1	1.86	1.72E-03
Pros35	1.86	5.95E-03
CG6299	1.85	5.75E-03
Prosbeta7	1.80	3.75E-03
CG15445	1.79	5.28E-03
qsm	1.78	1.13E-02
CG11378	1.78	2.50E-02
DnaJ-H	1.76	2.53E-03
CG17331	1.74	4.46E-03
Jheh1	1.73	8.66E-03
dgo	1.70	2.67E-02
IM3	1.69	3.05E-02
CG3348	1.69	4.28E-02
Prosbeta5	1.68	8.07E-03
CG5958	1.67	1.50E-02
Prosbeta1	1.65	6.22E-03
Hmu	1.65	1.08E-02
msd1	1.64	7.74E-03
CG4199	1.64	1.08E-02
cathD	1.63	9.09E-03
CG10208	1.62	1.45E-02
Gel	1.61	1.41E-02
GstE3	1.61	1.75E-02
Prosbeta2	1.60	6.70E-03
sev	1.58	2.74E-02
Prosalpha7	1.58	7.14E-03

Gene	$\log_2(foldchange)$	p-value
CG5167	1.57	2.87E-02
Lsm10	1.57	1.72E-02
Rpn9	1.57	9.83E-03
Rpn6	1.56	1.13E-02
Rpt1	1.55	8.58E-03
CG2046	1.55	6.56E-03
CG5384	1.55	1.59E-02
CG12795	1.54	7.79E-03
Pros29	1.53	1.19E-02
Roc1a	1.53	1.11E-02
Rpn12	1.52	2.12E-02
CG13779	1.51	8.89E-03
Cyp9f2	1.51	7.47E-03
Pros54	1.51	3.31E-02
Pros26	1.49	1.46E-02
Tsf1	1.49	3.31E-03
Pros25	1.47	1.99E-02
CG33099	1.46	3.51E-02
Pros45	1.46	1.90E-02
Cyp12d1-d	1.41	3.26E-02
CG11885	1.41	3.85E-02
p47	1.40	1.86E-02
Rpt4	1.39	4.25E-02
Uch-L3	1.39	2.20E-02
CG6218	1.36	2.05E-02
Sirt4	1.36	3.52E-02
PHGPx	1.36	1.86E-02
Rpn11	1.36	2.56E-02
Mov34	1.36	2.08E-02
CG12398	1.36	3.46E-02
CalpB	1.35	3.57E-02
Jheh2	1.32	3.59E-02
Clc	1.31	2.97E-02
Ube3a	1.31	3.51E-02
borr	1.28	4.07E-02
Irc	1.28	3.78E-02
Txl	1.27	2.78E-02
Rpn3	1.27	2.72E-02
CG42488	1.23	2.32E-02
TER94	1.21	3.78E-02
Ice	1.19	4.30E-02
CG4572	1.18	3.84E-02
Cyt-b5	1.17	3.81E-02
Prosbeta3	1.16	4.38E-02
CG4673	1.16	4.35E-02
CG13349	1.15	4.32E-02
CG9436	1.12	4.70E-02
SelG	1.11	4.04E-02

Supplementary Table 2. PCR primers.

Name	Sequence
RP49-f	CCGCTTCAAGGGACAGTATCTG
RP49-r	ATCTCGCCGCAGTAAACGC
lacZpromoter-f	ATCGCCCTTCCCAACAGTTGC
lacZpromoter-r	TTCTGGTGCCGGAAACCAGG
lacZreporter-f	TGCACATTTCAGGAGTACGGC
lacZreporter-r	GATTCGGCGCGACTGCTACC

Supplementary Table 3. ChIP-seq datasets read mapping statistics.

Library	Read Length	Uniquely mapped reads
Ovary shPiwi Rep1 H3K9me3	36	11,093,401
Ovary shPiwi Rep1 Input	36	23,783,156
Ovary shPiwi Rep1 Pol2	36	21,233,655
Ovary shWhite Rep1 H3K9me3	36	17,745,203
Ovary shWhite Rep1 Input	36	22,091,234
Ovary shWhite Rep1 Pol2	36	18,377,757
Ovary shPiwi Rep2 H3K9me3	36	22,467,219
Ovary shPiwi Rep2 H3K9me3 Input	36	14,843,946
Ovary shPiwi Rep2 Pol2	36	9,627,221
Ovary shPiwi Rep2 Pol2 Input	36	2,985,999
Ovary shWhite Rep2 H3K9me3	36	21,135,950
Ovary shWhite Rep2 H3K9me3 Input	36	16,619,035
Ovary shWhite Rep2 Pol2	36	5,731,448
Ovary shWhite Rep2 Pol2 Input	36	1,629,660

Supplementary Table 4. RNA-Seq datasets read mapping statistics. (TopHat 1.4.1 mappings)

Library	Read Length	Unique	Multi	Unique Splices	Multi splices
Ovary	50	19,868,793	3,249,894	2,021,378	31,552
Ovary shWhite Rep1	50	4,266,297	868,256	389,035	5,895
Ovary shPiwi Rep1	50	5,886,236	906,534	606,030	8,962
Ovary shWhite Rep2	50	10,345,357	1,186,659	607,786	18,881
Ovary shPiwi Rep2	50	12,764,829	1,393,823	1,177,886	25,302

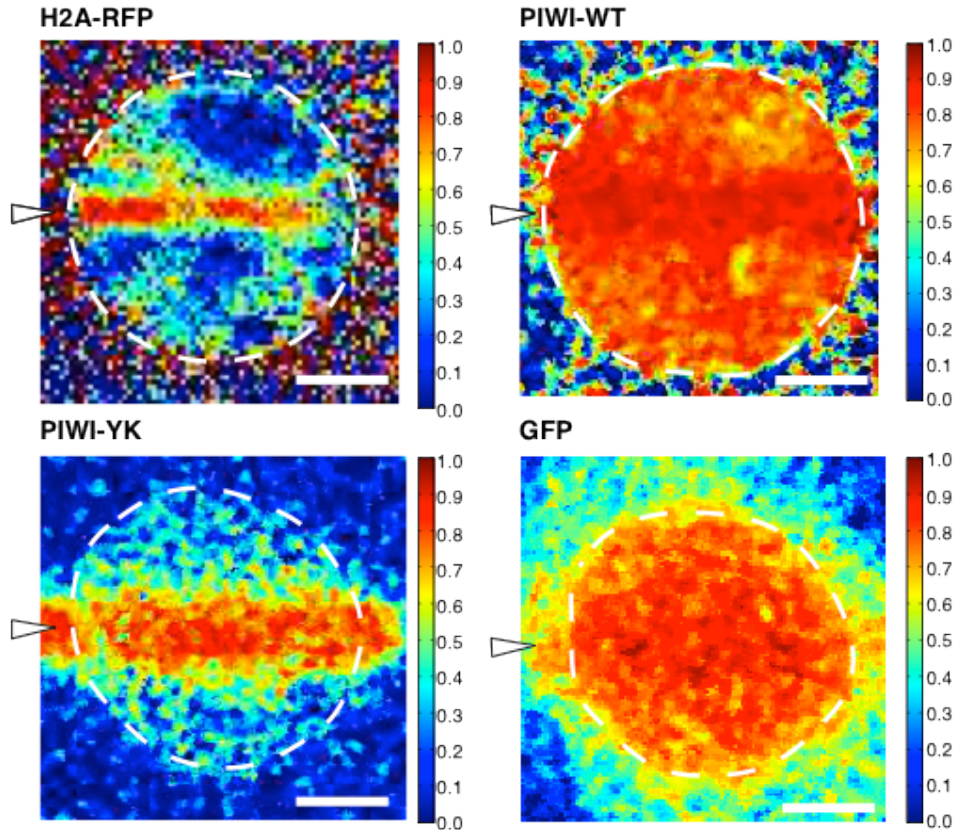
Supplementary Table 5. Repeat analysis mapping statistics. (whole genome with unlimited multimappers, zero mismatches)

Library	Read Length	Unique	Multi
Ovary shPiwi Rep1 H3K9me3	36	9,469,110	4,511,259
Ovary shPiwi Rep1 Input	36	20,029,978	2,042,023
Ovary shPiwi Rep1 Pol2	36	17,994,285	1,994,455
Ovary shWhite Rep1 H3K9me3	36	15,101,194	5,076,952
Ovary shWhite Rep1 Input	36	18,568,175	1,435,948
Ovary shWhite Rep1 Pol2	36	15,589,380	1,675,468
Ovary shWhite Rep1 RNA-seq	36	3,682,085	6,376,989
Ovary shPiwi Rep1 RNA-seq	36	5,119,512	5,808,312
Ovary shWhite Rep2 RNA-seq	36	8,658,005	4,005,709
Ovary shPiwi Rep2 RNA-seq	36	10,573,906	3,641,282
Ovary shPiwi Rep2 H3K9me3	36	13,315,195	3,808,164
Ovary shPiwi Rep2 H3K9me3 Input	36	13,489,170	3,501,374
Ovary shPiwi Rep2 Pol2	36	8,137,867	1,183,428
Ovary shPiwi Rep2 Pol2 Input	36	2,424,728	698,521
Ovary shWhite Rep2 H3K9me3	36	19,021,830	9,010,645
Ovary shWhite Rep2 H3K9me3 Input	36	12,018,516	5,698,668
Ovary shWhite Rep2 Pol2	36	4,858,338	824,157
Ovary shWhite Rep2 Pol2 Input	36	1,303,208	873,869

Supplementary Table 6. Repeat analysis mapping statistics. (consensus sequences)

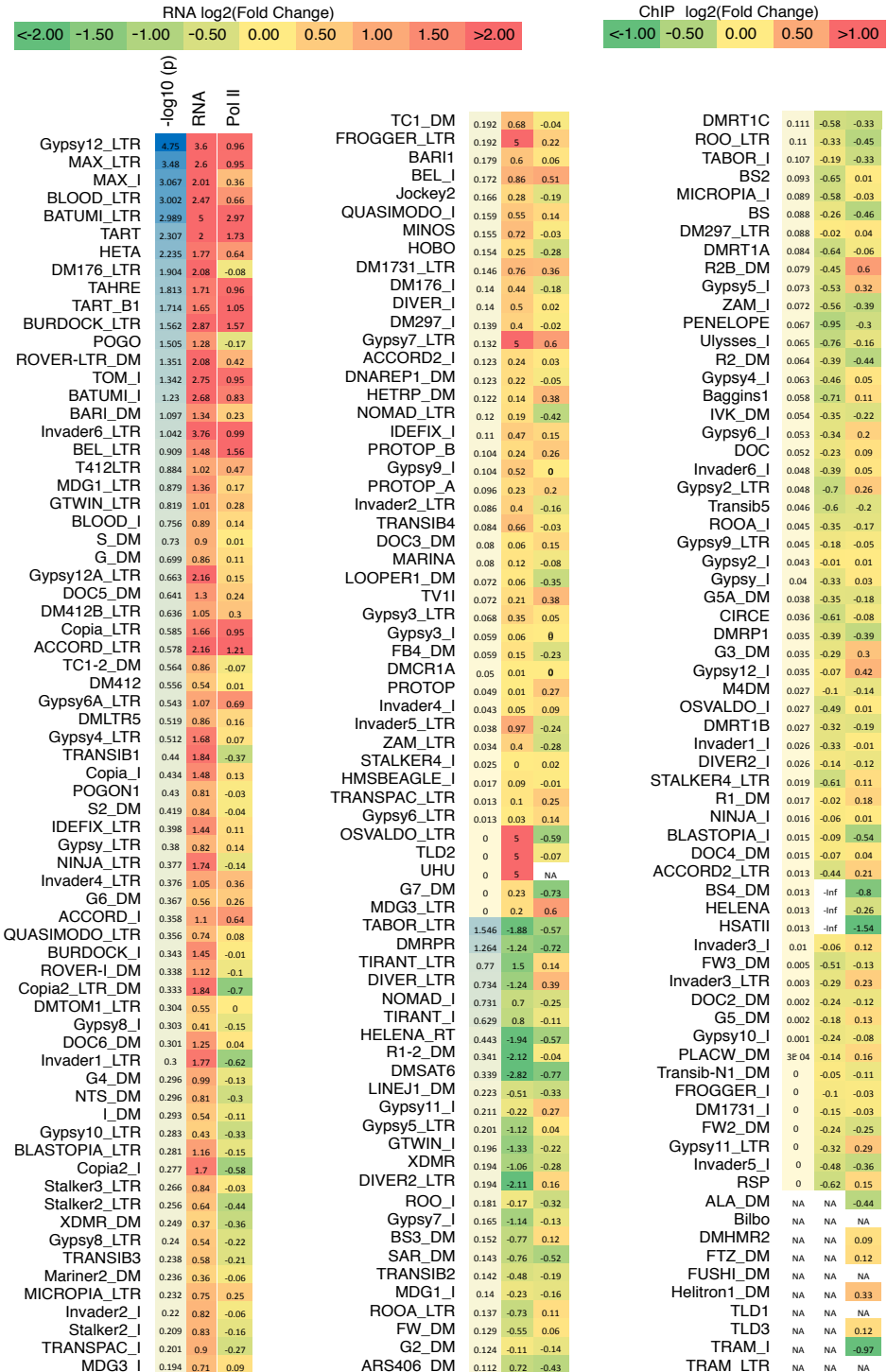
Library	Read Length	Unique	Multi
Ovary shWhite Rep1 RNA-seq	36	14,016	4,615
Ovary shPiwi Rep1 RNA-seq	36	39,413	9,692
Ovary shWhite Rep2 RNA-seq	36	15,309	7,910
Ovary shPiwi Rep2 RNA-seq	36	27,691	10,559
Ovary shPiwi Rep1 H3K9me3	36	2,720,971	283,437
Ovary shPiwi Rep1 Input	36	1,123,614	133,470
Ovary shPiwi Rep1 Pol2	36	515,368	109,711
Ovary shWhite Rep1 H3K9me3	36	3,208,049	318,559
Ovary shWhite Rep1 Input	36	739,854	83,425
Ovary shWhite Rep1 Pol2	36	346,044	74,633
Ovary shPiwi Rep2 H3K9me3	36	5,487,961	469,778
Ovary shPiwi Rep2 H3K9me3 Input	36	2,819,017	340,768
Ovary shPiwi Rep2 Pol2	36	380,988	79,937
Ovary shPiwi Rep2 Pol2 Input	36	318,557	38,475
Ovary shWhite Rep2 H3K9me3	36	5,556,191	463,857
Ovary shWhite Rep2 H3K9me3 Input	36	1,718,729	205,205
Ovary shWhite Rep2 Pol2	36	220,634	52,925
Ovary shWhite Rep2 Pol2 Input	36	174,554	25,171

Supplementary Figures and Figure Legends



Supplementary Figure S1. Fluorescence Loss in Photobleaching (FLIP) experiments indicate fast redistribution of most of nuclear Piwi and slower movement of the Piwi-YK mutant.

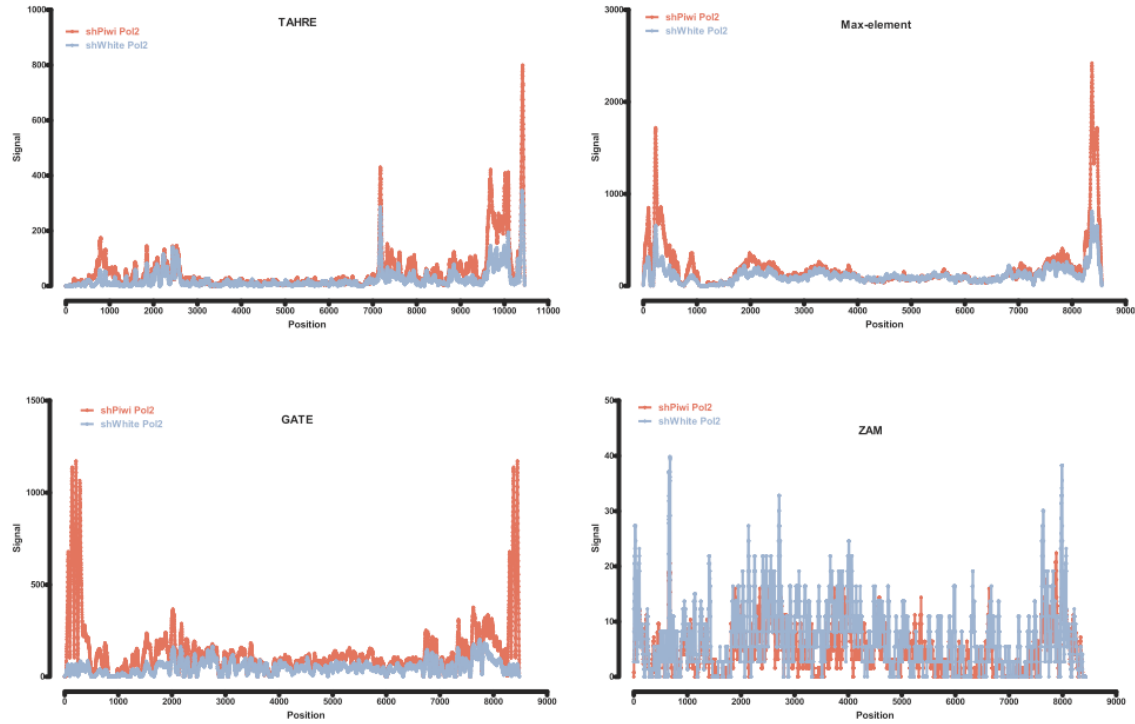
Amount of fluorescence decrease after 110 bleaching iterations for H2A-RFP, GFP-Piwi and GFP-Piwi-YK mutant and GFP in a nurse cell nucleus is shown. In each case significant fluorescence loss ($\geq 75\%$) across much of the nucleus, except for specific loci. GFP-Piwi-YK mutant exhibits far less change ($\leq 40\%$) in regions far from the site of bleaching. H2A-RFP control undergoes very little change in intensity away from the bleach region. Note that the apparent slower redistribution of free GFP is likely due to simultaneous nuclear import from the unbleached cytoplasmic pool. Bars = 5 μ m. Arrowheads indicate position of bleach stripe across the nucleus.



Supplementary Figure S2. Piwi regulates transposable element transcripts and RNA Polymerase II occupancy upon Piwi knockdown is shown. RNA-seq and ChIP-seq experiments were carried out in shWhite and shPiwi ovaries in two replicates. Differential expression was

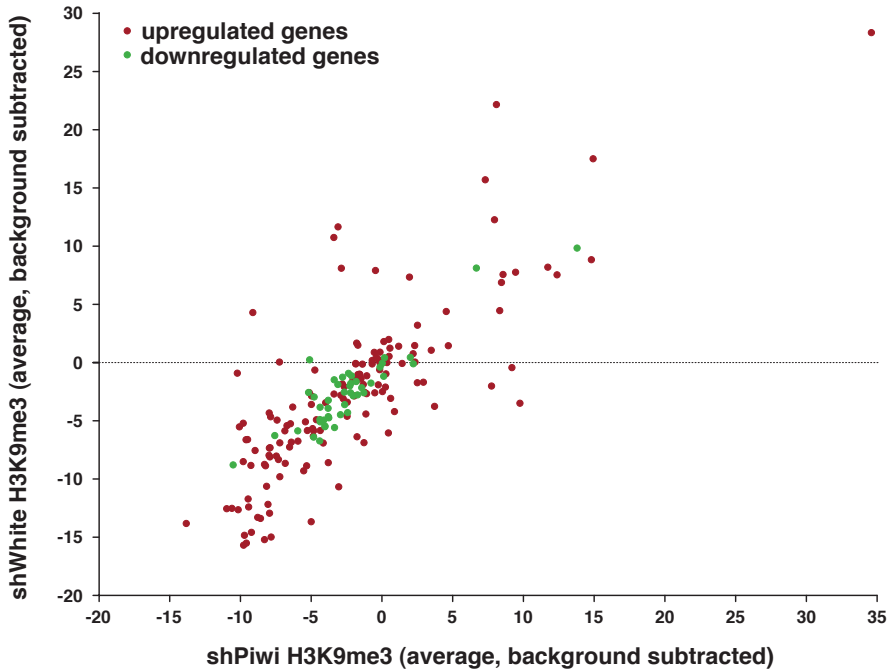
The change in the levels of transposable element transcripts and RNA Polymerase II occupancy upon Piwi knockdown is shown. RNA-seq and ChIP-seq experiments were carried out in shWhite and shPiwi ovaries in two replicates. Differential expression was

assessed using DESeq (see methods). The first column shows the statistical significance of the observed expression change (in $-\log_{10}(p\text{-value})$); up-regulated and down-regulated genes are sorted separately in order of decreasing significance. The second column shows the average change in RNA levels as defined by DESeq. The third column shows the average change in Pol II occupancy between the two replicate experiments.



Supplementary Figure S3. Piwi depletion increases RNA Pol II association with promoters of transposable elements.

RNA polymerase II ChIP-Seq signal over the consensus sequences of selected transposable elements in the control (shWhite) and Piwi-depleted (shPiwi) ovaries. RNA polymerase II occupancy increases in the promoter regions (LTRs) of transposons upon germline knockdown of Piwi. Transposons expressed in somatic follicular cells such as ZAM are not affected.



Supplementary Figure S4. Piwi depletion does not alter H3K9me3 occupancy over differentially expressed genes upon Piwi knockdown.

Scatter plot indicating average H3K9me3 mark levels upon Piwi depletion (shPiwi) and control (shWhite) over genes that were previously identified in the RNAseq experiments to be differentially expressed upon Piwi knockdown. (red: up-regulated genes, green: down-regulated genes). The average signal of two biological replicas was taken after subtraction of the corresponding input signals.

Chapter III

**PIRNA-INDEPENDENT RECRUITMENT OF PIWI TO RNA
TRANSCRIPTS IS NOT SUFFICIENT TO TRIGGER
TRANSCRIPTIONAL SILENCING**

Part of this work has been submitted for publication as:

Chen, A. C. et al. “Su(Var)2-10, a novel component of the piRNA-induced transcriptional silencing complex, controls co-transcriptional repression of piRNA targets”. (Submitted).

Supplementary Tables

Supplementary Table S1. Oligonucleotide sequences used in experimental procedures.

Name	Sequence
RP49-f	CCGCTTCAAGGGACAGTATCTG
RP49-r	ATCTCGCCGCAGTAAACGC
Primer A-f	GTGACTGTGCGTTAGGTCTG
Primer A-r	TGAAGTGGTGGTTGTTCACGG
Primer B-f	ATGGTGAGCGAGCTGATTAAGG
Primer B-r	TGAAGTGGTGGTTGTTCACGG
Primer C-f	TCAGAGGGGTGAACCTCCC
Primer C-r	CTCCCAGCCGAGTGTTCCT
Primer D-f	GGCCGACAAAGAGAGACCTACG
Primer D-r	CCAGTTGCTAGGGAGGTCTG
Luciferase-f	CGTCGCCAGTCAAGTAACAA
Luciferase-r	TTTCTTGCCTCGAGTTTCC

Chapter IV

ZUCCHINI-DEPENDENT PIRNA PROCESSING IS TRIGGERED BY
RECRUITMENT TO THE CYTOPLASMIC PROCESSING MACHINERY
SUPPLEMENTAL MATERIAL

This work was first published as:

Rogers, A. K. et al. (2017). "Zucchini-dependent piRNA processing is triggered by recruitment to the cytoplasmic processing machinery". In: *Genes & Development* 31: 1-12.
doi: 10.1101/gad.303214.117.

Supplementary Tables

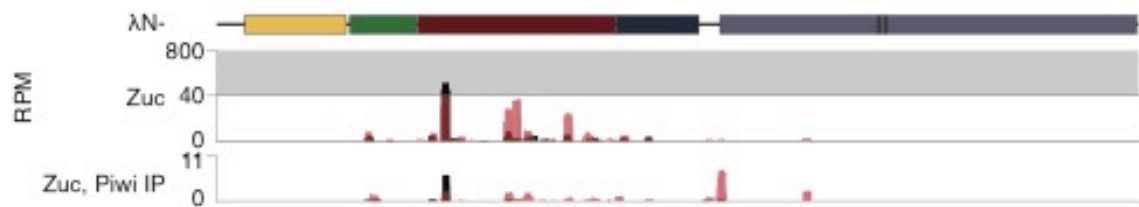
Supplementary Table S1. Library mapping statistics.

#Indicates which replicate is plotted on tracks

Mapping to:	DM3 genome	Reporter						42AB	Rebase	miRNA	Endo-siRNA
Sample	All reads	All reads	5'U reads	Specific reads	Specific 5'U reads	All sense reads	Specific reads	5'U 23-29nt reads	Unique reads	All reads	
AN-GFP (TJ-gal4) replicate 1 #	2344077	45	17	34	14	44	46879	957552	510848	3034	
AN-GFP (TJ-gal4) replicate 2	6333387	92	41	61	25	84	123904	2525139	1503061	8681	
AN-Yb (TJ-gal4) replicate 1 #	4849740	1797	1477	1130	960	1795	120766	1965418	1446366	7145	
AN-Yb (TJ-gal4) replicate 2	9291798	1195	907	664	506	1188	244535	3456252	3060715	14563	
AN-Piwi (TJ-gal4) replicate 1 #	6371453	1031	641	806	486	997	136398	2404211	1511076	4554	
AN-Piwi (TJ-gal4) replicate 2	8359291	900	213	605	146	298	188777	3322242	2363988	12010	
AN-GFP (MT-gal4) replicate 1 #	12046162	129	74	66	30	115	378358	4452673	3129830	11894	
AN-GFP (MT-gal4) replicate 2	5956459	50	32	27	17	48	189674	2522173	1586086	6601	
AN-Cuff (MT-gal4) replicate 1 #	11050911	143	74	87	40	132	247942	4679320	3736766	14756	
AN-Cuff (MT-gal4) replicate 2	101027	4	0	4	0	3	2433	37282	8189	14	
AN-THOC5 (MT-gal4) replicate 1 #	2848142	126	63	86	38	122	35499	1345862	686334	4473	
AN-THOC5 (MT-gal4) replicate 2	13246	1	0	1	0	1	171	3733	6134	27	
AN-Zuc (MT-gal4) replicate 1 #	7021497	6288	931	6231	910	6282	100692	2075995	2998093	18089	
AN-Zuc (MT-gal4) replicate 2	6672189	8458	1099	8394	1084	8450	101182	2164831	2441202	13050	
AN-Piwi (MT-gal4) replicate 1 #	14003310	2820	1732	1916	1044	2808	302992	5291372	3104376	8390	
AN-Piwi (MT-gal4) replicate 2	10501272	854	502	662	378	849	172803	3851723	4056208	18948	
AN-Arx (MT-gal4) replicate 1 #	4977488	60	38	46	32	52	159264	1886641	1313932	4254	
AN-Arx (MT-gal4) replicate 2	1720575	25	18	13	10	22	40744	571814	558210	3576	
AN-Egg (MT-gal4) replicate 1 #	11654274	587	159	487	126	573	238818	3195948	4731174	25383	
AN-Egg (MT-gal4) replicate 2	6326648	490	162	264	77	422	137834	1939413	1980572	12613	
AN-Panx (MT-gal4) replicate 1 #	6407104	100	64	69	46	94	187024	2479665	1894213	8683	
AN-Panx (MT-gal4) replicate 2	2302003	104	42	70	28	99	45065	638213	845587	4952	
AN-Aub (MT-gal4) replicate 1 #	5898318	674	377	599	337	670	150375	2146550	1634008	5480	
AN-Aub (MT-gal4) replicate 2	6461928	811	437	809	436	803	174663	2535271	1623796	8451	
AN-Arm (MT-gal4) replicate 1 #	3824887	2145	1768	1465	1261	2143	87874	1297263	1223310	4634	
AN-Arm (MT-gal4) replicate 2	9266056	5320	3957	3469	2699	5310	240435	3642518	2989403	8157	
AN-Piwi GFP-Piwi IP replicate 1 #	18781682	7948	4391	5868	2976	7915	698560	8786907	1348207	2960	
AN-Piwi GFP-Piwi IP replicate 2	7791490	5688	2838	1163	1459	5677	220880	3619280	211387	527	
AN-Aub Piwi IP replicate 1 #	9028977	2048	856	1720	646	2037	25954	4759656	134642	599	
AN-Aub Piwi IP replicate 2	7151788	1537	873	1103	541	1531	213405	3360445	384500	1084	
AN-Zuc GFP-Piwi IP replicate 1 #	8943934	555	232	4871	142	552	313258	5202163	266054	721	
AN-Zuc GFP-Piwi IP replicate 2	5197468	483	186	404	116	480	117748	2211612	1017994	2166	
AN-Piwi sh-White replicate 1 #	9138738	2326	1439	1995	1220	2313	227634	4008593	2067270	7110	
AN-Piwi sh-White replicate 2	5781800	2284	1457	1904	1196	2276	135017	2448831	1223758	4072	
AN-Piwi sh-Panx replicate 1 #	6321423	2190	1317	1821	1069	2183	230065	2577153	1654769	5076	
AN-Piwi sh-Panx replicate 2	1128098	436	284	366	239	433	40054	428881	262232	740	
AN-Piwi sh-Egg replicate 1	9978444	1799	1074	1443	815	1787	235554	3639827	3237148	11168	
AN-Piwi sh-Egg replicate 2 #	5861571	1345	837	1137	682	1332	117890	1725870	1866563	9216	
AN-Piwi sh-Cuff replicate 1 #	7348197	4298	2764	3637	2280	4287	35247	1816550	2841750	9819	
AN-Piwi sh-Cuff replicate 2	4926517	3207	2253	2561	1753	3184	19665	1056932	2047340	6096	
AN-Piwi sh-THOC5 replicate 1 #	3973885	1304	765	1134	645	1304	88488	1619213	1104102	3141	
AN-Piwi sh-THOC5 replicate 2	3606026	1311	789	1067	615	1311	76982	1310241	1019678	3451	
AN-Piwi sh-Zuc replicate 1 #	2087785	76	13	64	12	73	19094	399880	821114	5028	
AN-Piwi sh-Zuc replicate 2	514916	40	12	27	9	34	4863	105125	179913	1600	
AN-Piwi sh-Arm (MT-gal4) replicate 1 #	4245306	82	23	66	15	80	27284	756263	2395362	9589	
AN-Piwi sh-Arm (MT-gal4) replicate 2	4389133	121	40	94	34	112	29821	790865	2457437	12015	
AN-Piwi sh-Vasa replicate 1 #	7560513	867	506	697	393	861	73696	1813136	4011742	18746	
AN-Piwi sh-Vasa replicate 2	2594545	407	205	339	159	401	20695	438649	1257932	8632	
AN-Piwi sh-Krimper replicate 1 #	10530300	1273	829	955	592	1227	166110	3080713	4466063	23662	
AN-Piwi sh-Krimper replicate 2	1368207	132	76	92	53	125	13462	251310	564699	4629	
AN-Piwi sh-Aub replicate 1 #	374891	106	70	87	59	104	3207	69579	185468	771	
AN-Piwi sh-Aub replicate 2	6348155	1674	1046	1331	812	1670	66845	1334711	3043905	15943	
AN-Piwi sh-AGO3 replicate 1 #	3759996	2755	1743	2337	1410	2750	58243	1036373	1317907	3494	
AN-Piwi sh-AGO3 replicate 2	3830634	2240	1333	1837	1057	2225	47351	874200	1568077	6265	
AN-GFP (MT-gal4) NaiO4 treated replicate 1 #	1265932	30	15	21	10	30	47426	756081	4648	720	
AN-GFP (MT-gal4) NaiO4 treated replicate 2	1562407	104	52	92	42	101	50061	941412	5063	986	
AN-Zuc (MT-gal4) NaiO4 treated replicate 1 #	380848	16	9	14	8	16	10154	239434	1825	494	
AN-Zuc (MT-gal4) NaiO4 treated replicate 2	67210	6	3	6	3	6	1658	39726	1354	72	
AN-Piwi (MT-gal4) NaiO4 treated replicate 1 #	283137	52	33	36	24	50	6702	171507	641	126	
AN-Piwi (MT-gal4) NaiO4 treated replicate 2	443150	68	37	58	28	68	10785	254763	2534	167	
AN-Aub (MT-gal4) NaiO4 treated replicate 1 #	3980774	381	230	263	155	378	135912	2293238	6477	1879	
AN-Aub (MT-gal4) NaiO4 treated replicate 2	175259	14	8	14	8	14	5824	85906	746	116	
AN-Arm (MT-gal4) NaiO4 treated replicate 1	48081	7	2	3	2	7	1512	16912	517	32	
AN-Arm (MT-gal4) NaiO4 treated replicate 2	1706046	1817	1461	550	438	1812	51069	1039851	12395	2031	
AN-GFP-Piwi with GFP reporter #	8963238	509	250	505	199	482	157730	3181335	3083185	17602	
AN-GFP with GFP reporter #	4582258	50	27	22	17	30	111071	1948988	1100320	6146	
AN-FLAG-Piwi with GFP reporter #	7203731	501	253	420	217	474	112806	2143920	3265805	16256	
AN-FLAG with GFP reporter #	12885683	321	122	140	58	300	320330	4566240	4531623	24346	
AN-FLAG-Piwi with mKate2 reporter #	9840772	1881	1345	1584	1126	1874	253903	4457571	1814397	8643	
AN-FLAG with mKate2 reporter #	4126774	67	35	50	28	63	121205	1673304	1028499	3430	

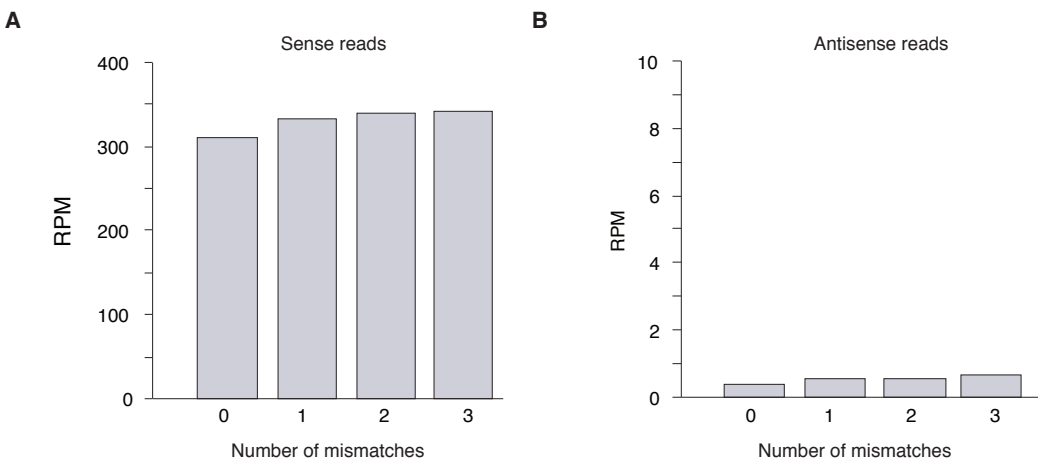
Supplementary Table S2. Oligonucleotide sequences used in experimental procedures.

Oligonucleotide name	Sequence
DM_Thoc5_shRNA-F	CTAGCAGTGGTGAAGCACAAGATCAAATAGTTATTCAGCATATTGATCTTGCTTCACCGCG
DM_Thoc5_shRNA-R	AATTCCGGTGAAGCACAAGATCAAATATGCTGAATAACTATTGATCTTGCTTCACCACTG
RP49-F	CCGCTTCAGGGACAGTATCT
RP49-R	ATCTCGCGCAGTAACG
Panoramix-F	GACGAGGGCGCAGATGATAA
Panoramix-R	TCATTCTGCGAACTGGCACT
Egg-F	ATGGAGGTAAAGGCCCTGAT
Egg-R	TGGCTTCCGTGTTCTCCC
Cutoff-F	CTGAAGAGGGCCATGCAAGA
Cutoff-R	GCTGGTCATCTTAATGCCG
Thoc5-F	TGAGCTCAAGCAGGAAC TG
Thoc5-R	TGCGCTTAGCTCCATTCCA
Zucchini-F	ATTGTTCCGTGCGGAATGTG
Zucchini-R	TGATCCGGATAATCACGCCG
Armi-F	CGTGTGAAAACCAAGGAGG
Armi-R	AGCAACAAATCTGCCTTGG
Vasa-F	TGAGTGATGTTCTGGACGC
Vasa-R	AATGTCATGATTTCTGGACGC
Krimper-F	CTGGCTGAAAACAGGGAAC
Krimper-R	TCCCCTGGGAGGCAATAGGA
Aub-F	TCCGCTACTTCTCCACCGTA
Aub-R	TCACCTCGCTGTTACCACC
AGO3-F	AGGAATGGCAAACCCCCAC
AGO3-R	CCCGAGAAGATGCGAGTGT
FISH Probes for mKate2	TGTTCTCCTTAATCACGCTG
	TCCATGTACAGCTTCATGTG
	TCGGATGTGCACTTGAAGTG
	CTTGATTCATGGTCTGGG
	GTCGAAGGGCGAAGGGGAGAG
	TACATGAAGCTGGTAGCCAG
	GTTGATGAAGGTTTGCTGC
	TCGGGGAGGACTGCTAAA
	ITCGTATGTTGACTCTCT
	CTTGACGTTGAGATGAGGC
	CGTTGGATGGGAAGTTTCACC
	AGTGTTTCTCTGCATCAC
	TCAAGTTGCAGATCAGGTGG
	TTCTTGATCTGTATGTTGG
	CATCTTGAGGTTCTAGCGG
	TGTCACATAGTAGACGCCG
	CTCCTTGATTCTTCAGTC
	TCGACGTAGGTCTTTGTC
	TAGGGAGGTGCGAGTATCTG
	AACAAAGGAACCGATCCCT
	AAAGGAACCTTGGTCGAGC
	CAATTGGCCCTTTTCAGG
	TGCATGAATATCCTCCAGTG
	CCACAAAGGAACCTTGGTC
	ATCAATTGGCCCTTTCA
	TCGAGTGCATGAATATCCTC
	CGTTACGTTAACGTTAACGT
	ATGTTATCAAGCTCTCGAG
	TACTCTGACCATGGGTTA
	GTGTTCTCAACTTCAAAGGC
	AATGTCAGGTTAACAGGG
	GCTTTAACTGAGTTCTTC
	ATTGCTAATTGCTAATTGCT
	CTTCTCGTTTGAAGTCAGC
	GTGCCTTACAAATACTTGCA
	AGCCGTCGGTGGTCTATAAA
	AGTTACATGACGAGCCTAA
	ATGTTCAATTGGGTTCAACC
	ATCTTCCCCATTGATAATAA
	ATTACTTTGCTACCTGAGGG
	CTTAGGACTCTTATTGCA
	AAGGTCAAAGGGCCAGATT
	ATTGAACCCAAATGCACCTG
	GGGATGGGAAAGTGTTTAT
	TGCGGTATTCTCATTATTG

Supplementary Figures and Figure Legends

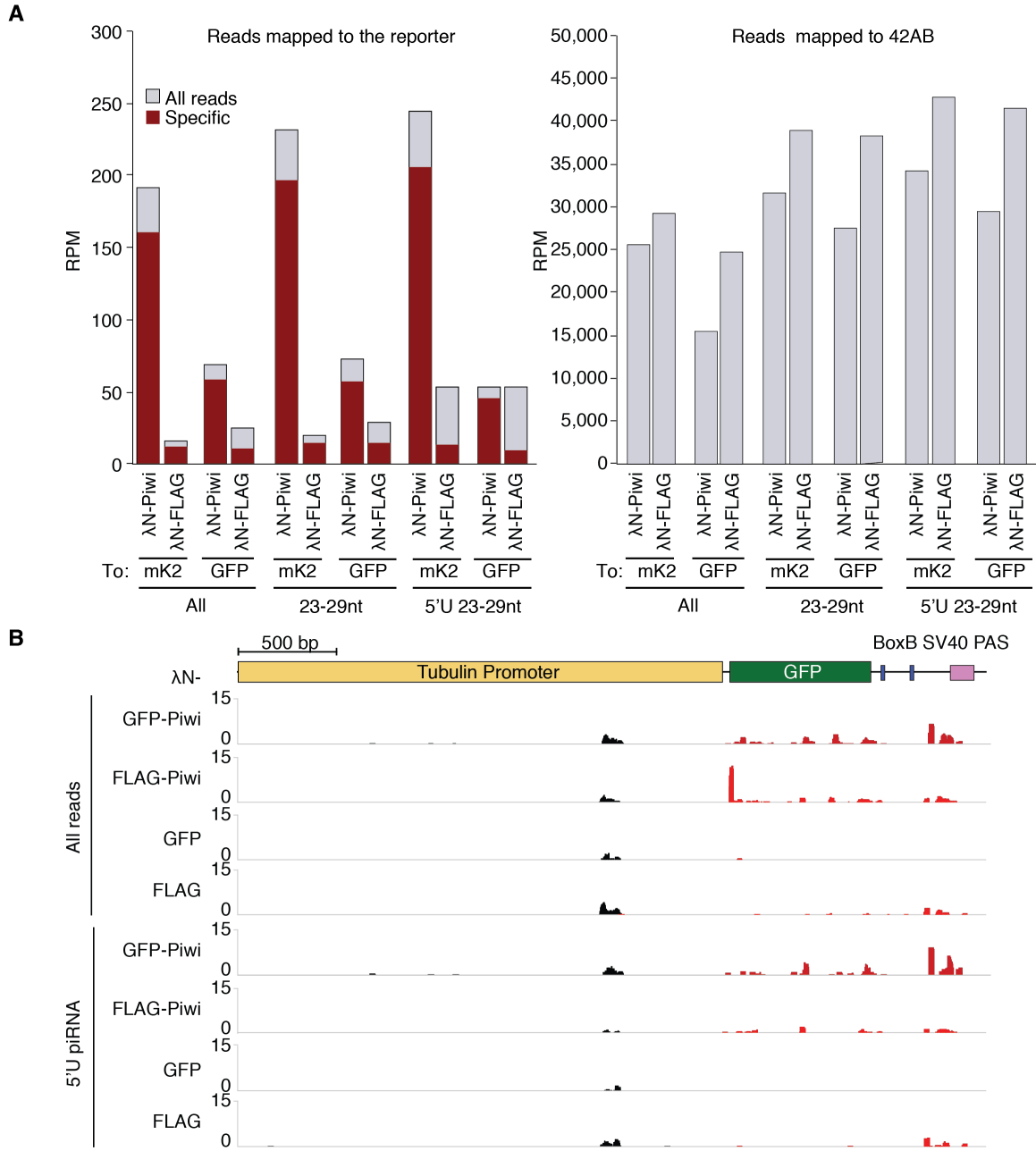
Supplementary Figure S1. Upon Zuc tethering, reporter derived sequences that are 25-28nt in length (black) map along the whole body of the reporter, whereas 22-23nt reads (red) map predominantly at the 5' region of the reporter transcript.

Shown are profiles for reads specifically mapping to the reporter, normalized to all reads mapping to the DM3.



Supplementary Figure S2. Recruitment of Piwi to the reporter triggers production of piRNAs in sense orientation.

A) Tethering of λN -Piwi to the reporter results in piRNA-sized (25-28nt) reads in the sense orientation. Shown are RPMs of small RNA from 19-30nt total ovarian RNA calculated for 25-28nt reads mapping to the DM3 genome. **B)** Tethering of λN -Piwi to the reporter does not result in piRNA-sized (25-28nt) reads in the antisense orientation. Shown are RPMs of small RNA from 19-30nt total ovarian RNA calculated for 25-28nt reads mapping to the reporter in antisense orientation, allowing for 0, 1, 2, or 3 mismatches, normalized to total 25-28nt reads mapping to the DM3 genome.

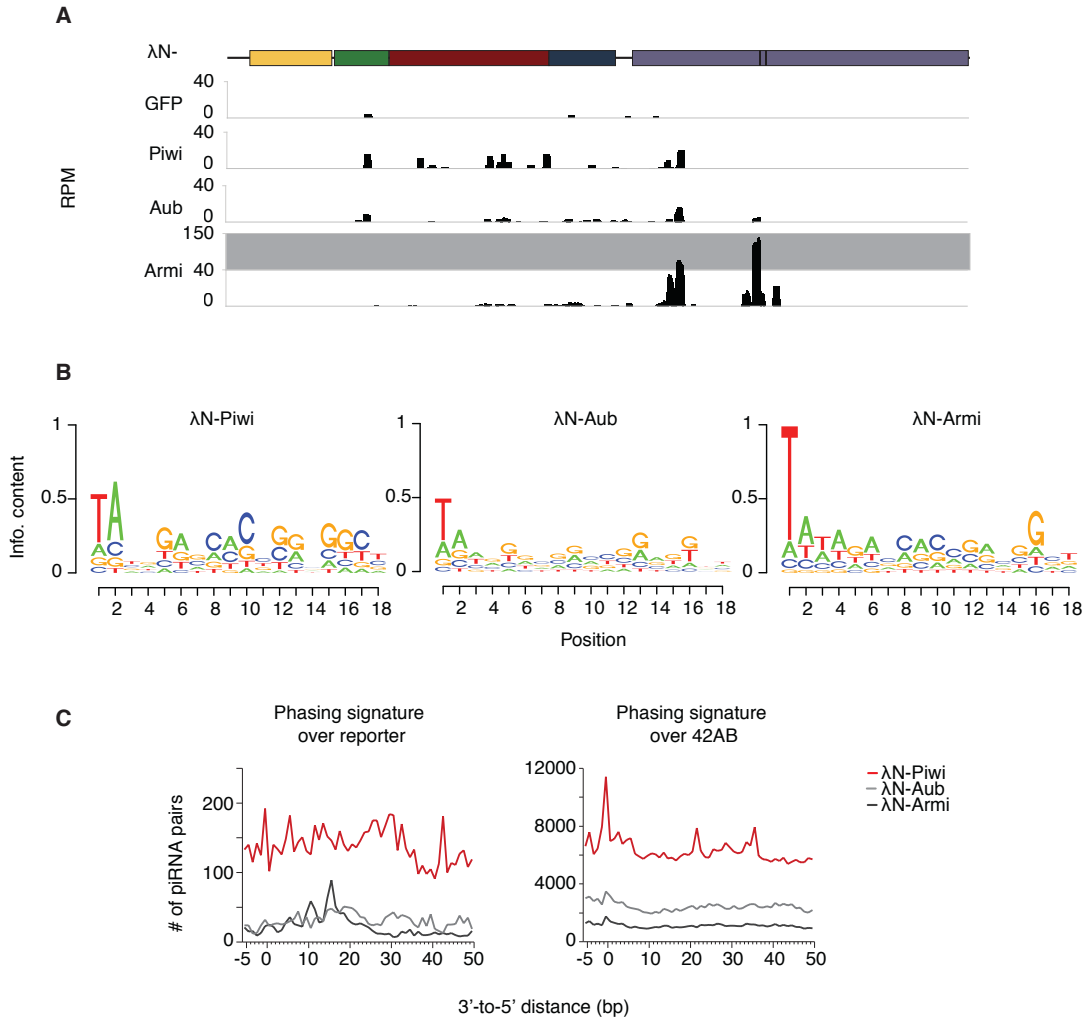


Supplementary Figure S3. Production of piRNAs upon Piwi tethering is independent of the λN-Piwi fusion construct, as well as the reporter sequence and genomic location.

A) Tethering of λN-FLAG-Piwi to the mKate2-4xBoxB, or to the Tubulin-GFP-BoxB reporter, results in piRNA production from the reporter. In the left graph, RPMs of small RNA-seq libraries from size selected total RNA from ovaries are shown. RPMs were calculated for reads mapping to the reporter specifically or non-specifically (allowed to map to the DM3 genome) normalized to total reads mapping to the DM3 genome. Size selected or 5'U reads mapping to the reporter were normalized to corresponding reads

mapping to the DM3. On the right, RPMs calculated for reads specifically mapping to 42AB, normalized to reads mapping to the DM3 genome are shown for the same dataset.

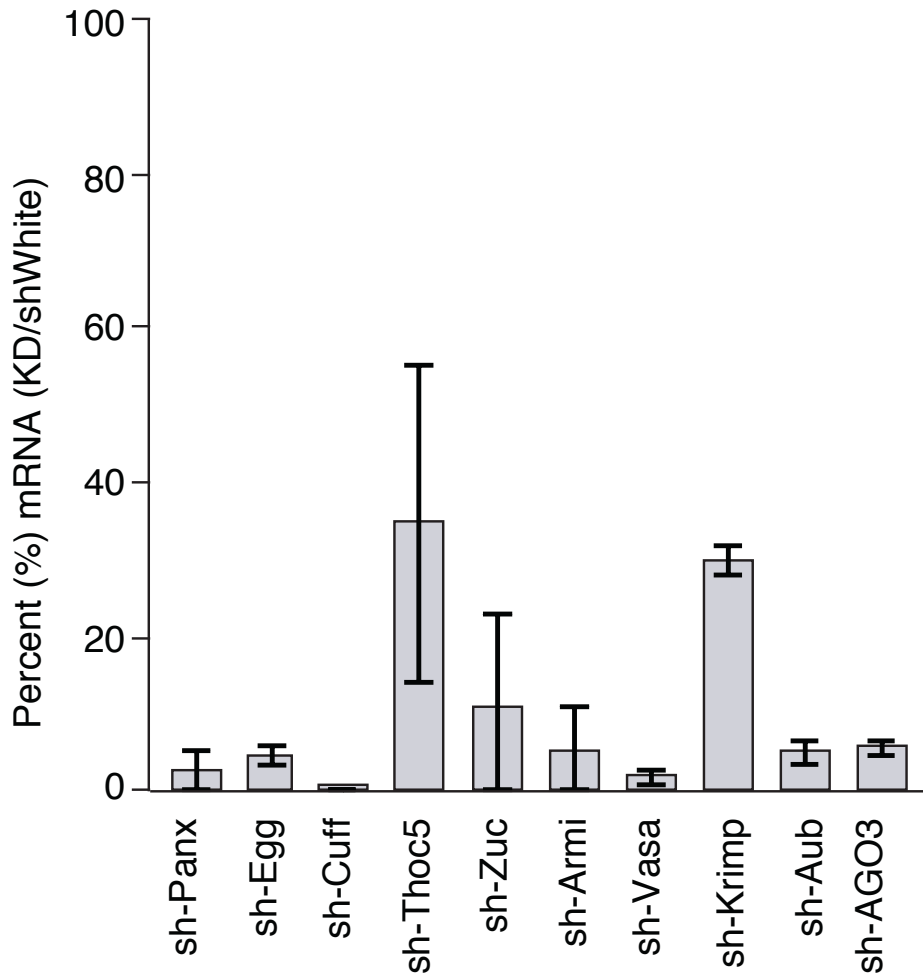
B) Recruitment of Piwi to the Tubulin-GFP-BoxB reporter results in piRNAs mapping along the entire reporter sequence. Shown are profiles for all reads (black) and reporter-specific reads (red) mapping to the reporter, normalized to all reads mapping to the DM3 genome. As a control, neither λ N-GFP nor λ N-FLAG tethering resulted in pIRNAs.



Supplementary Figure S4. Recruitment of Piwi, Aub, or Armi to the reporter triggers production of piRNAs resistant to NaIO₄ treatment.

A) Shown are profiles for all reads mapping exclusively to the reporter, normalized to all mapping to the DM3 genome in libraries cloned after NaIO₄ treatment of RNA. **B)** Reporter-derived small RNAs generated upon Piwi, Aub, or Armi tethering have a 1U bias. Shown are weblogos for all reads mapping exclusively to the reporter in libraries cloned after NaIO₄ treatment. **C)** Reporter-derived small RNAs generated upon Piwi, Aub, or Armi tethering are not phased. Shown is the calculated 3' to 5' distance between reads mapping to the reporter (left) and reads mapping to 42AB (right).

Percent mRNA remaining after KD, normalized to shW & RP49



Supplementary Figure S5. Percent mRNA remaining after knockdown of piRNA pathway component mRNAs in the tethering system.

Knockdown efficiency of each mRNA was measured using RT-qPCR from total ovarian RNA, normalized to RP49 and to RNA levels in the control (shWhite). Error bars indicate standard deviation of biological replicates (n=2).

Chapter V

IDENTIFYING DIRECT PROTEIN INTERACTIONS WITH PIWI USING
A HETERLOGOUS CELL CULTURE ASSAY SUPPLEMENTAL
MATERIAL

This work will be submitted for publication as:

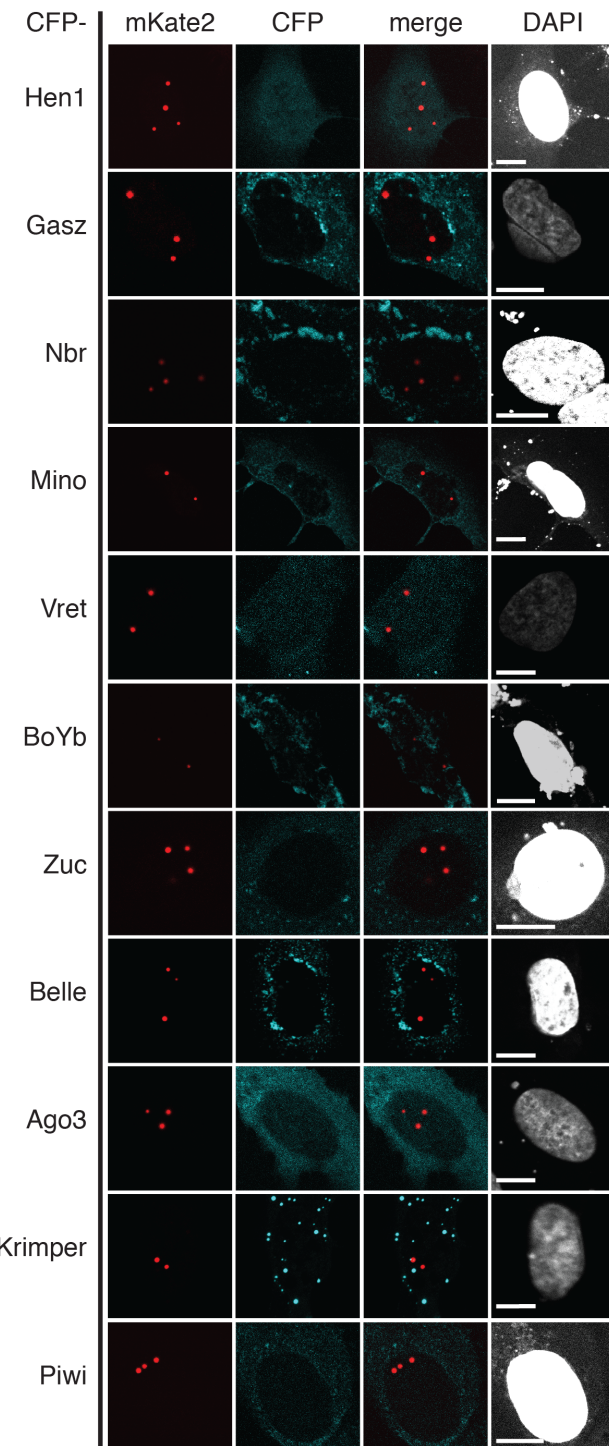
Rogers, A. K. et al. "Mago and Arp6 identified as novel *Drosophila* Piwi interactors using a heterologous two-hybrid system". (Submitted)

Supplementary Tables

Supplementary Table S1. Colocalization analysis statistics.

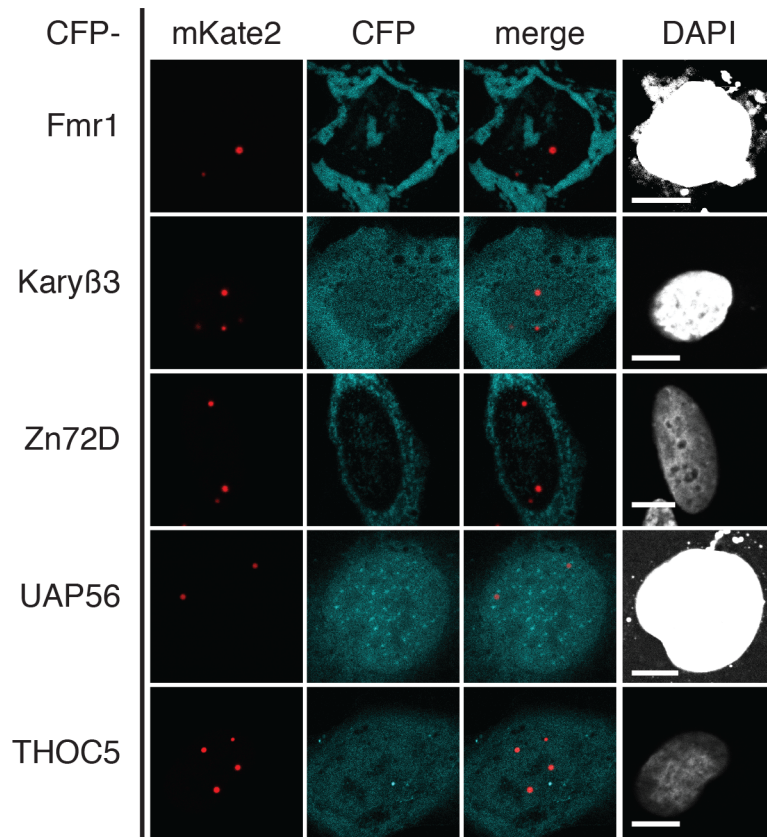
Supplementary Table S2. Oligonucleotide sequences used in experimental procedures.

Name	Sequence
Asterix-TOPO-F	CACCATGGTTATTGCCGTACAACAAG
Asterix-TOPO-R	CTACTGGCGCCTGAGTATGGC
RnpS1-TOPO-F	CACCATGGCGCTGCCAGAGTCT
RnpS1-TOPO-R	CTAACGAGAGCTGCACTGCTATT
Mago-TOPO-F	CACCATGTCCACGGAGGACTTTACCTAC
Mago-TOPO-R	TTATATGGGCTTGATCTTGAATGCAG
Nxt1-TOPO-F	CACCATGGACAGCGAT TTGAAAGCCAAG
Nxt1-TOPO-R	TCAGACCTCCTGCATTGGTAGC
Kary β 3-TOPO-F	CACCATGGCAGCGATCAGGCCATT
Kary β 3-TOPO-R	TTAGGCAGGGAGCCACGTTG
Arp6-TOPO-F	CACCATGGCCAACGCTGTGGTGGT
Arp6-TOPO-R	TTACCGCTGATTGATAACCTGGAAAC
His2AV-TOPO-F	CACCATGGCTGGCGTAAAGCAGGCAA
His2AV -TOPO-R	TTAGTAGGCCTGCGACAGAATGAC
Crm-TOPO-F	CACCATGGAGGAACGTCCAAGCAGCC
Crm-TOPO-R	CTAACCTTCTCCTGCTGCTGCAGC
Zn72D-TOPO-F	CACCATGGCCAACAACAACGCG
Zn72D-TOPO-R	TTATCCTGCAGAGAGAGAAGCTGCC
Panoramix-TOPO-F	CACCATGGAAGCTCGATGAAGCTAGAGG
Panoramix -TOPO-R	CTATGGCTGTCGACCCTTTATTATTG
Caf1-105-TOPO-F	CACCATGAAGTGCAGATAACCGAGATTTC
Caf1-105-TOPO-R	CTACTCTAAAAGTTCTTTTGATTTGGC
H1-TOPO-F	CACCATGTCTGATTCTGCAGTTGCAACGTCC
H1-TOPO-R	TTACTTTGGCAGCGTAGTCTCG
YL-1-TOPO-F	CACCATGGCTGCCCGATCACG
YL-1-TOPO-R	TTAGTTATCTCCGTTTGTGGCAGCTG
Acnius-TOPO-F	CACCATGAGACGTCGAGCGAGCG
Acnius-TOPO-R	CTAGTAACGTCTCGCTCCGCTCG
Δ MLS-Zuc-TOPO-F	CACCATGTTGATTACCAAATAATTATGAAACAAATTGAG
Δ MLS-Zuc-overlap-R	TTCTCTGCTGCCTGGCCAGACTGCACCAGCTTCAAATC
Δ MLS-Zuc-overlap-F	TCGGCCAGCGCAGCAGAGAAGGCAAGCCGCTGCAC
Δ MLS-Zuc-TOPO-R	CTTGAGCTGGATTGGCTCCCC
Fmr1-TOPO-F	CACCATGGAAGATCTCCTCGTGGAAAGTTCG
Fmr1-TOPO-R	TTAGGACGTGCCATTGACCAAGG
Cp190-TOPO-F	CACCATGGGTGAAGTCAAGTCCGT
Cp190-TOPO-R	TTATAGCTCCTTCGCCG
E(z)-TOPO-F	CACCATGAATAGCACTAAAGTGCCGC
E(z)-TOPO-R	TCAAAACAATTCCATTTCACGCTCT
Hsp83-TOPO-F	CACCATGCCAGAAGAAGCAGAGACC
Hsp83-TOPO-R	TTAACGACCTCCTCCATGTGG
Nbr-TOPO-F	CACCATGGCACGCCAGAGCACAT
Nbr-TOPO-R	TCACTAACATGGGCACCCCG
Tudor-SN-TOPO-F	CACCATGGCACAGCAGCGAACAC
Tudor-SN-TOPO-R	TTAGCGGAACTCGGCGCAT
Corto-TOPO-F	CACCATGACGATGGCCGCTGTTAT
Corto-TOPO-R	TCACACGTTGAGCAGGAGATCT
Esc-TOPO-F	CACCATGAGCAGTGATAAAGTGAAAAACGGCAA
Esc-TOPO-R	TCAGATGGAAGTTGTTGCTGCGGTT
KpnI-lacI-F	ACATGGTACCATGGCGGAGCTGAATTACATTCCA
lacI-mKate2-R	TCCTTAATCAGCTCGTCACCATCTGCCGCTTCCAGTCG
lacI-mKate2-F	AGCGGGCAGATGGTGAGCGAGCTGATTAAGGAGA
mKate2-SphI-R	ACATGCATGCCGTGGACCGGTCTGTG
XbaI-lacI-F	ACATTCTAGAATGGCGGAGCTGAATTACATTCCA
lacI-mKate2-att-NotI-R	CTAATGCGGCCCATAGTGA

Supplementary Figures and Figure Legends

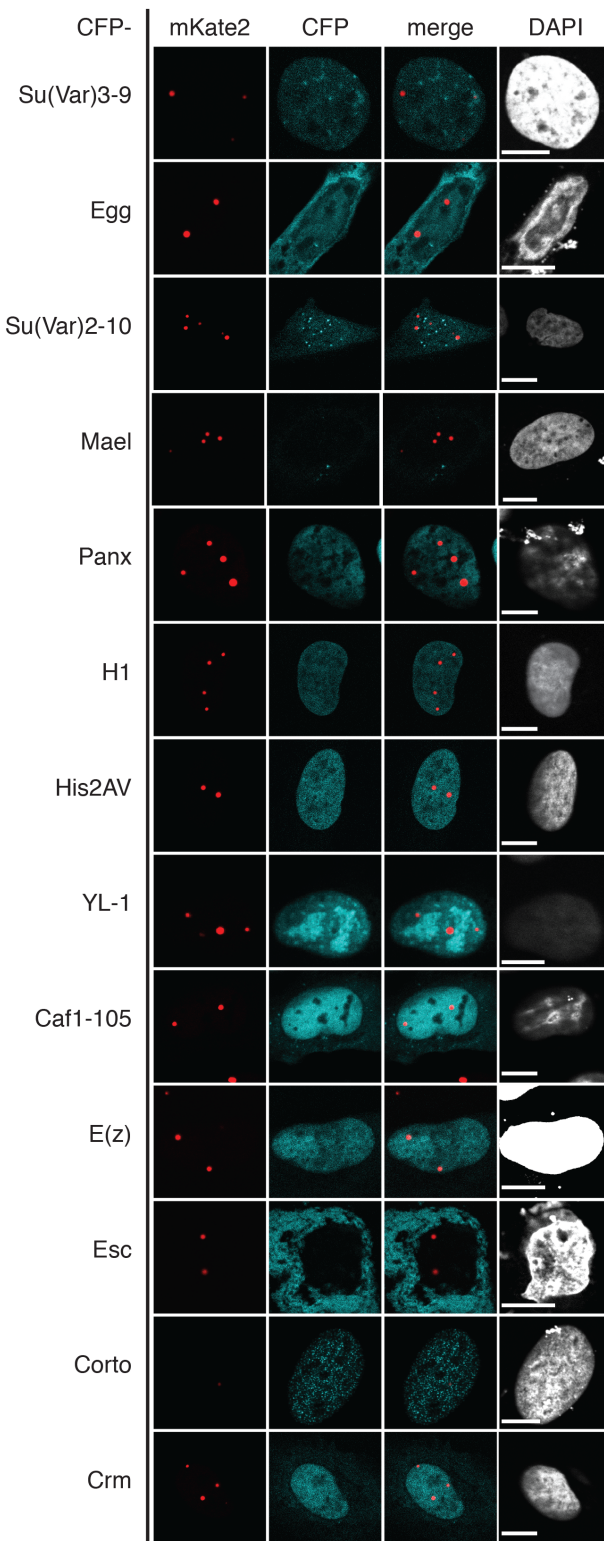
Supplementary Figure S1. Piwi does not directly interact with many nuage localized factors involved in piRNA biogenesis.

LacI-mKate2-Piwi foci did not recruit CFP-tagged Hen1 (p-value=0.096; std=0.124; n=5), Gasz (p-value=0.154; std=0.344; n=5), Nibbler (Nbr) (p-value=0.00; std=0.00; n=5), Minotaur (Mino) (p-value=0.018; std=0.040; n=5), Vreteno (Vret) (p-value=0.212; std=0.172; n=5), BoYb (p-value=0.062; std=0.139; n=5), Zucchini (Zuc) (p-value=0.196; std=0.210; n=5), Belle (p-value=0.028; std=0.063; n=5), Argonaute3 (Ago3) (p-value=0.010; std=0.017; n=5), Krimper (p-value=0.00; std=0.00; n=5), or Piwi (p-value=0.162; std=0.362; n=5). Representative images are shown. Scale bar represents 10 μ m.



Supplementary Figure S2. Piwi does not directly interact with several factors involved in transcript export from the nucleus.

LacI-mKate2-Piwi foci did not recruit CFP-tagged Fmr1 ($p\text{-value}=0.00$; $\text{std}=0.00$; $n=5$), Kary β 3 ($p\text{-value}=0.154$; $\text{std}=0.238$; $n=5$), Zn72D ($p\text{-value}=0.00$; $\text{std}=0.00$; $n=5$), UAP56 ($p\text{-value}=0.002$; $\text{std}=0.004$; $n=5$), or THOC5 ($p\text{-value}=0.030$; $\text{std}=0.051$; $n=5$). Representative images are shown. Scale bar represents 10 μm .



Supplementary Figure S3. Piwi does not directly interact with many nuclear factors involved in chromatin modification.

LacI-mKate2-Piwi foci did not recruit CFP-tagged Su(Var)3-9 (p-value=0.00; std=0.00; n=5), Eggless (Egg) (p-value=0.060; std=0.129; n=5), Su(Var)2-10 (p-value=0.006; std=0.005; n=5), Maelstrom (Mael) (p-value=0.056; std=0.114; n=5), Panoramix (Panx) (p-value=0.222; std=0.361; n=5), H1 (p-value=0.092; std=0.200; n=5), His2AV (p-value=0.00; std=0.00; n=5), YL-1 (p-value=0.0008; std=0.018; n=5), Caf1-105 (p-value=0.136; std=0.266; n=5), E(z) (p-value=0.338; std=0.368; n=5), Esc (p-value=0.00; std=0.00; n=5), Corto (p-value=0.486; std=0.459; n=5), or Cramped (Crm) (p-value=0.608; std=0.380; n=5). Representative images are shown. Scale bar represents 10 μ m.